In-situ fabrication of 3D self-supported porous Ni-Mo-Cu catalyst for efficient hydrogen evolution reaction

Fang Miao[a,1], Peng Cui[b*,1], Shijie Yu[b], Tao Gu[a]

[a] *College of Materials Science and Engineering, North University of China, Taiyuan, 030051, China*

[b] *Jiangsu Key Laboratory of Advanced Metallic Materials, School of Materials Science and Engineering, Southeast University, Nanjing, 211189, China*

[1]Authors contributed equally to this work

*Corresponding author: Tel: +0086 025 52091093

Email address: cuipeng1993@hotmail.com

Mail address: School of Materials Science and Engineering, Southeast University, Nanjing, 211189, China

Table S1
Chemical compositions (EDS) and the samples.

Sample	Ni, at%	Cu, at%	Mo, at%
I	55	45	-
II	52	43	5
III	52	41	7

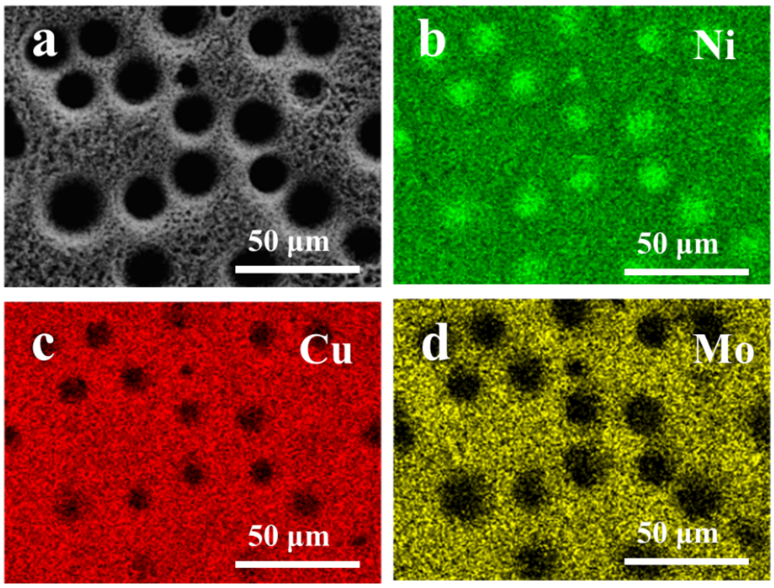

Fig. S1 (a) SEM image and (b-d) corresponding elemental mapping images of Ni, Cu, and Mo.

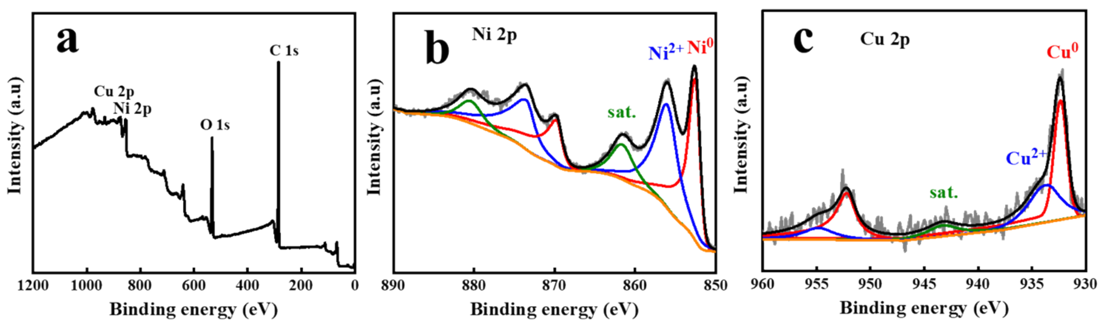

Fig. S2 XPS spectra of (a) survey, (b) Ni 2p, (c) Mo 3d, and (d) Cu 2p of sample I.

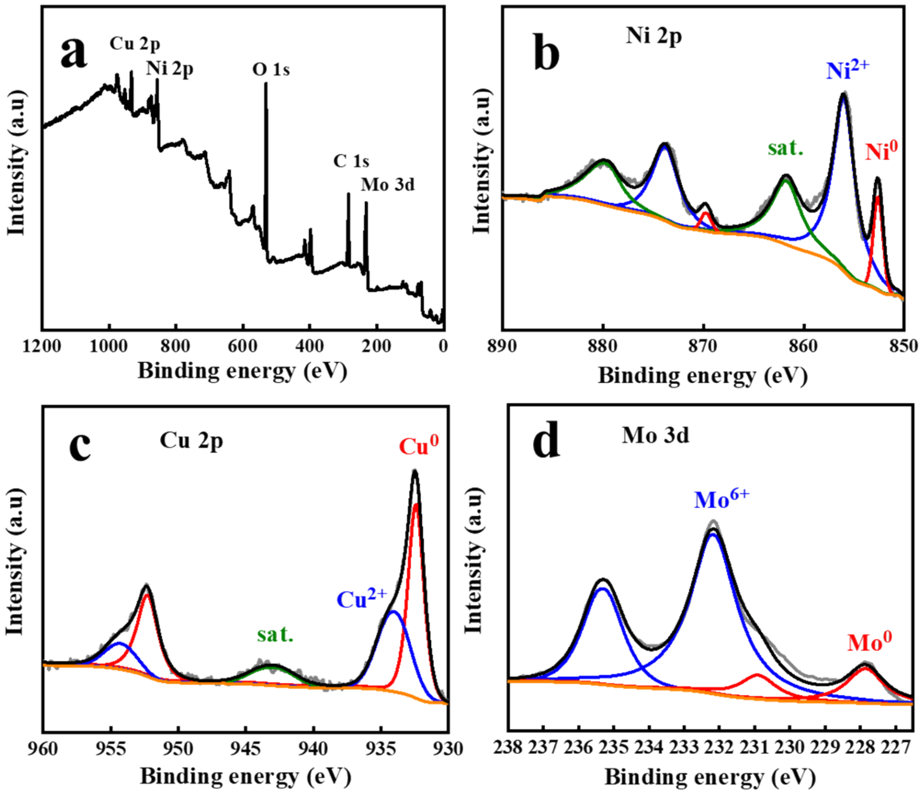

Fig. S3 XPS spectra of (a) survey, (b) Ni 2p, (c) Mo 3d, and (d) Cu 2p of sample III.

Table S2

The binding energy values of Ni^0 $2p_{3/2}$, Cu^0 $2p_{3/2}$, and Mo^0 $3d_{5/2}$ of three samples.

Sample	Ni^0 $2p_{3/2}$	Cu^0 $2p_{3/2}$	Mo^0 $3d_{5/2}$
I	852.3	932.2	-
II	852.6	932.4	227.6
III	852.5	932.5	227.7

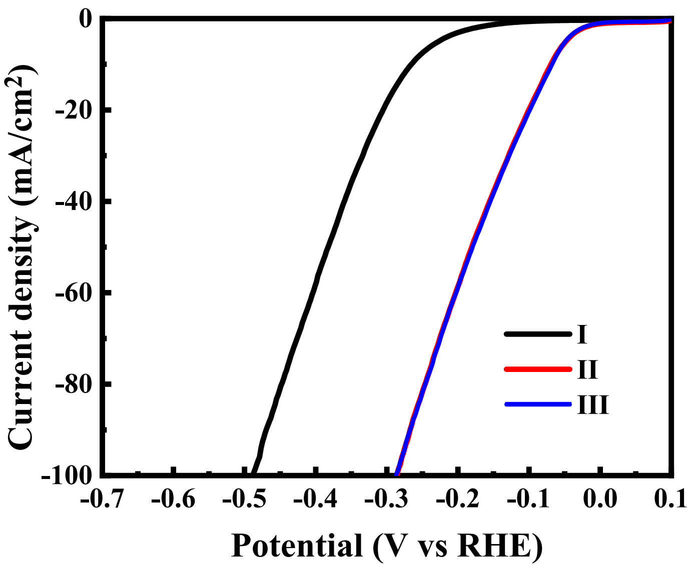

Fig.S4 LSV curves before IR compensation of the sample I, II and III.

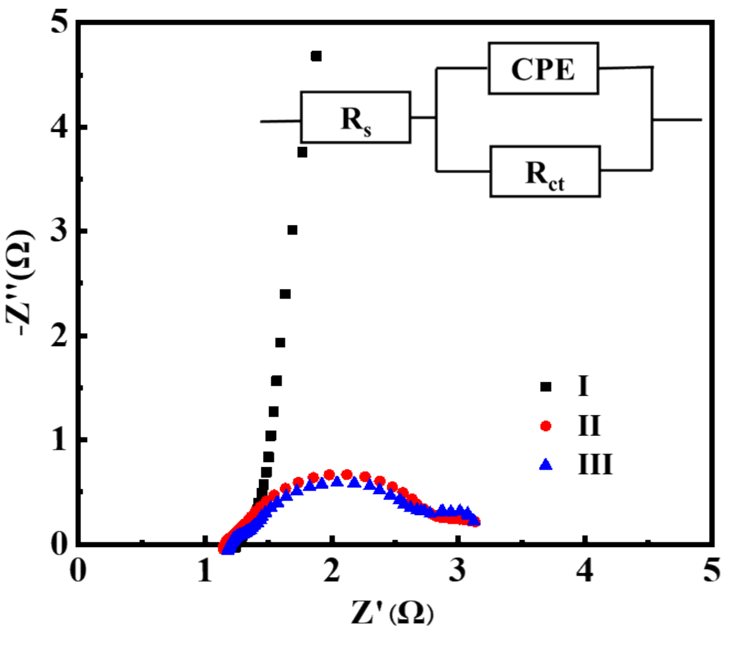

Fig. S5 EIS measurements for the samples, the inset is the equivalent circuit mode.

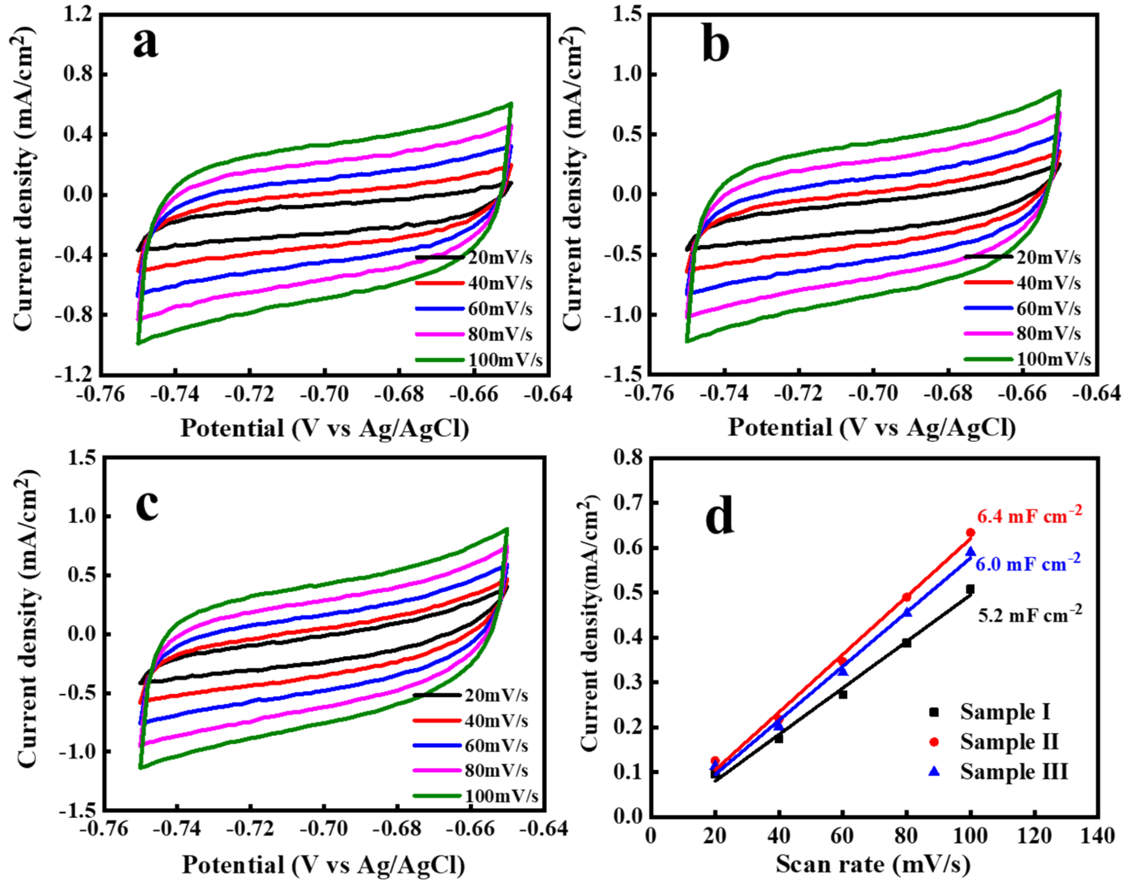

Fig. S6 CV-scan curves of (a) sample I, (b) sample II, and (c) sample III in 1M KOH; (d) C_{dl} measurements for the samples.

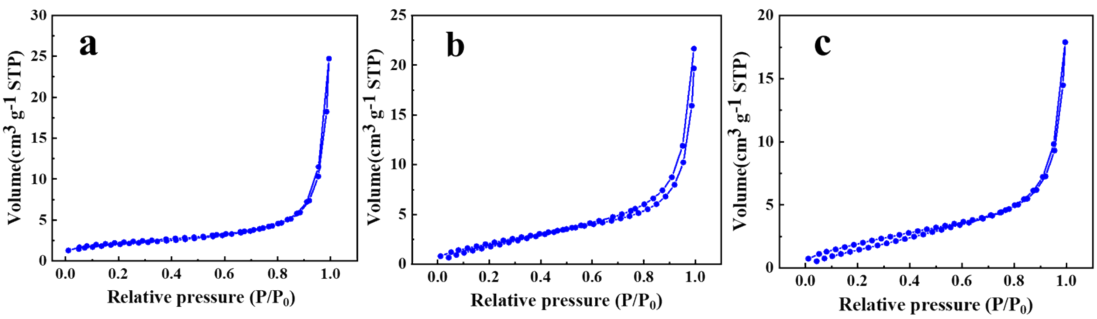

Fig. S7 The N_2 adsorption/desorption isotherm curves of (a) sample I, (b) sample II, and (c) sample III.

Table S3

Comparison of the HER performance of NiMoCu and other some catalysts.

Catalysts	Overpotential (mV) at j =10 mA cm^{-2}	Tafel slope (mV/dec)	References
Ni-Mo-Cu	70	53	this work
3DOM-Ni_2P/Fe_xP	106	81	[1]
$Ni(OH)_2$/NiMoS	180	81	[2]
NiCoP/NPC	128	70	[3]
NiCu	76	72	[4]
CoP	101	45.1	[5]
H-B/Ru-Fe	110	76.1	[6]
CoP/N-doped carban	167	57	[7]
NiCoP@SSM	138	74	[8]

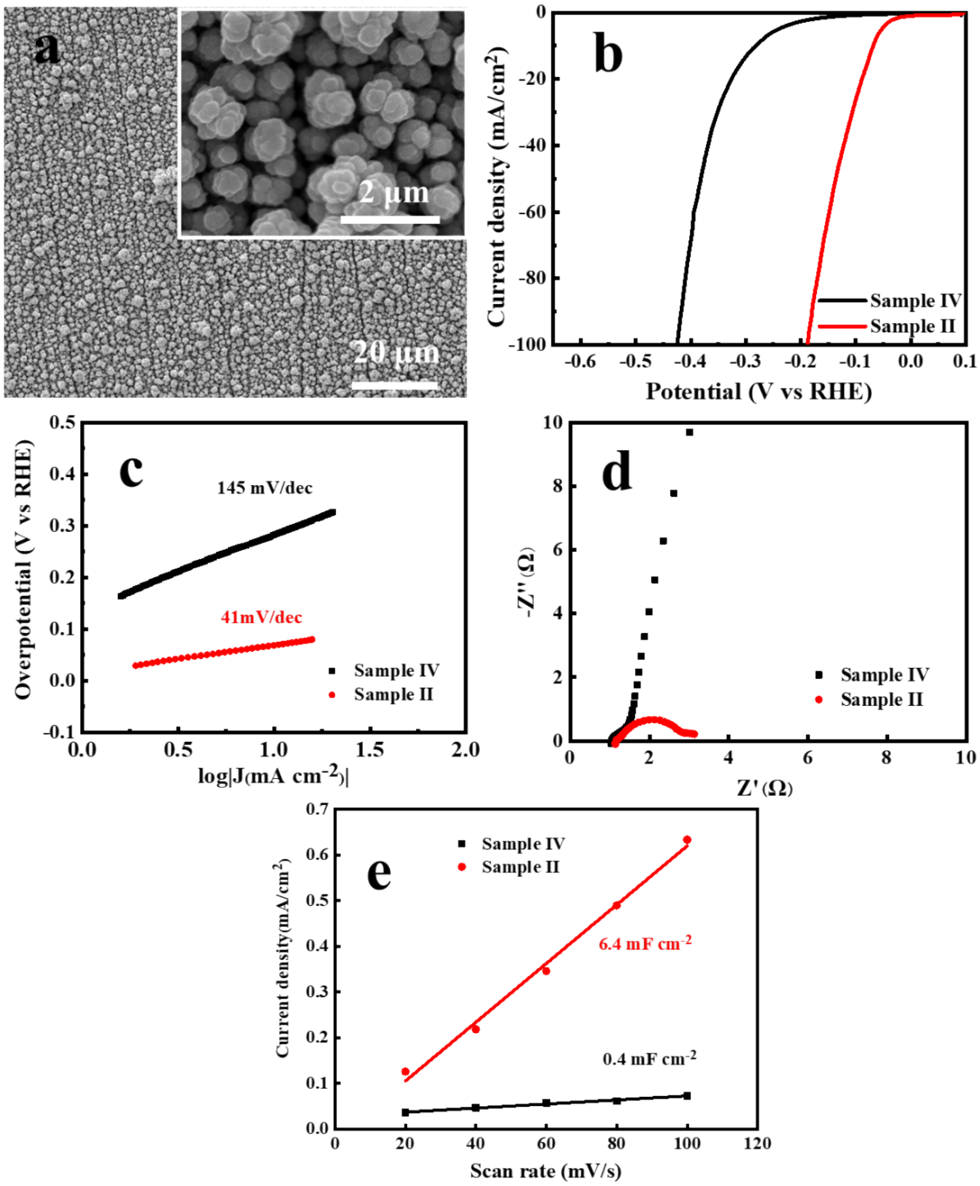

Fig. S8 (a) SEM images of sample IV. (b) LSV curves, (c) Tafel plots, (d) EIS measures, (e) C_{dl} of sample II and sample IV.

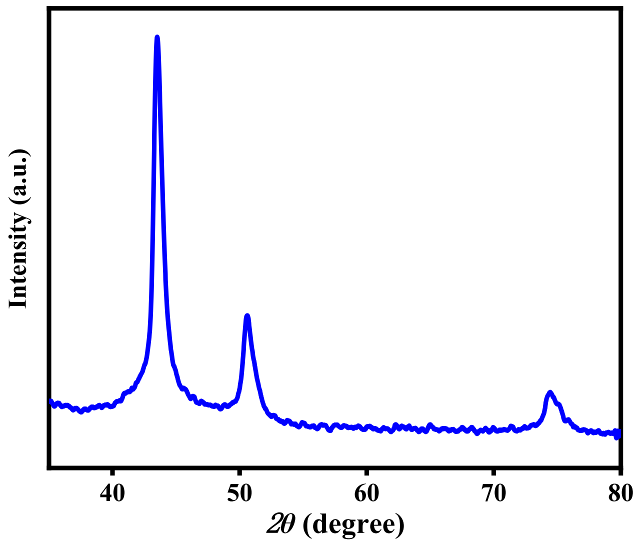

Fig. S9 XRD pattern of sample II after stability test.

Table S4
Chemical compositions (EDS) and sample II after stability test.

Sample	Ni, at%	Cu, at%	Mo, at%
II	51	44	5

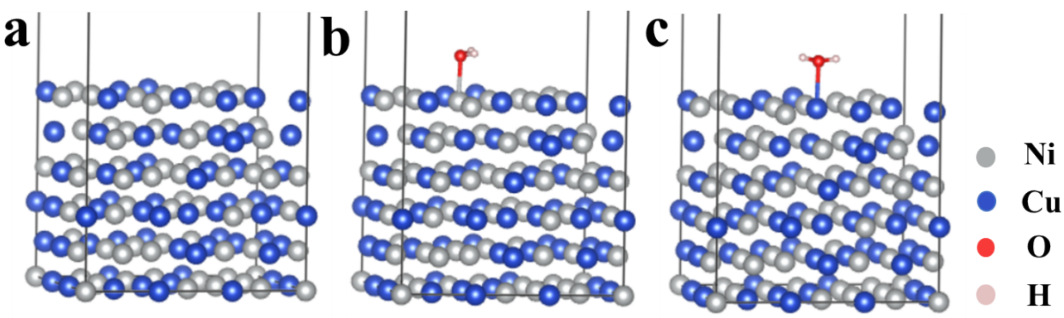

Fig. S10 (a) The optimized structure of sample I (NiCu), and the H_2O molecule adsorbed on different sites of (b) Ni and (c) Cu. The values of adsorption energy of H_2O molecule on Ni site and Cu site are -0.54 eV and -0.45 eV.

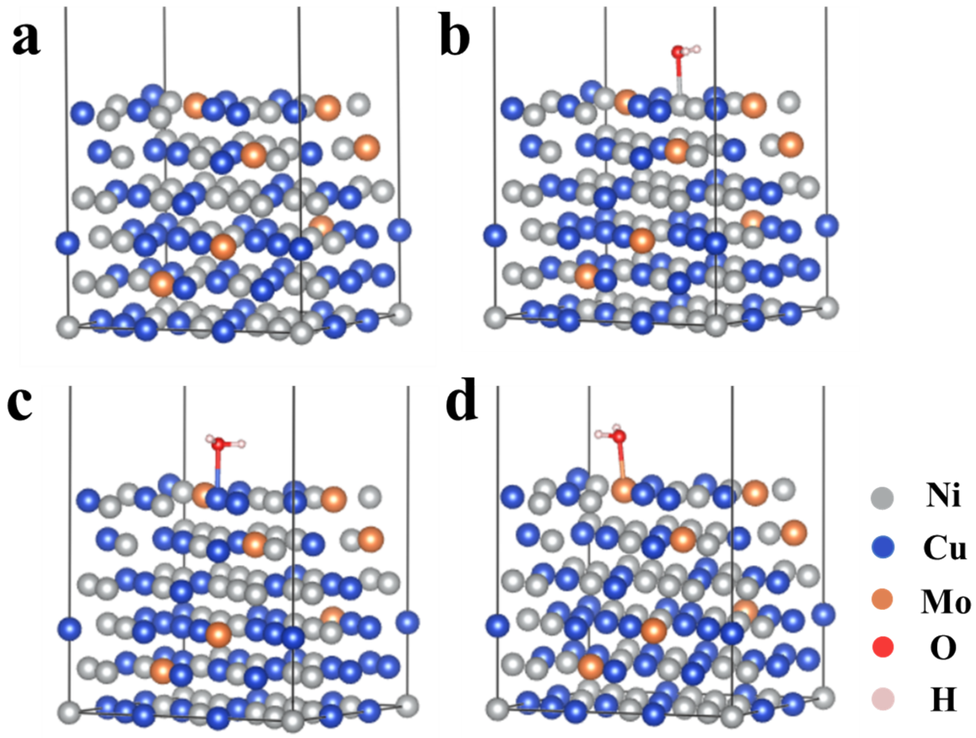

Fig. S11 (a) The optimized structure of sample II (NiMoCu), and the H_2O molecule adsorbed on different sites of (b) Ni, (c) Cu, and (d) Mo. The values of adsorption energy of H_2O molecule on Ni site, Cu site, and Mo site are -0.35 eV, -0.44 eV, and -1.01 eV.

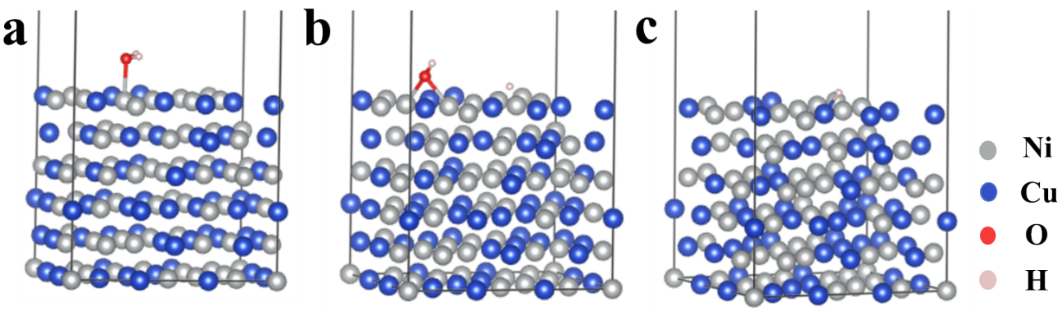

Fig. S12 Different stages of catalytic pathways of Sample I for HER.

References

[1] Cao WJ, Zhao RH, Liu GH, Wu LL, Li JD. Three-dimensional ordered macroporous design of heterogeneous nickel-iron phosphide as bifunctional electrocatalyst for enhanced overall water splitting[J]. Appl Surf Sci. 2023; 607: 154905.

[2] Yang CM, Zhou LH, Yan T, Bian YJ, Hu YJ, Wang CT, Zhang YT, Shi YM, Wang DJ, Zhen YZ, Feng F. Synergistic mechanism of $Ni(OH)_2$/NiMoS heterostructure electrocatalyst with crystalline/amorphous interfaces for efficient hydrogen evolution over all pH ranges. J Colloid Interf Sci. 2022; 606:1004-1013.

[3] Yi MJ, Lu BB, Zhang XT, Tan YB, Zhu ZY, Pan ZC, Zhang JH. Ionic liquid-assisted synthesis of nickel cobalt phosphide embedded in N, P codoped-carbon with hollow and folded structures for efficient hydrogen evolution reaction and supercapacitor [J]. Appl Catal B-Environ. 2021; 283: 119635.

[4] Niu JJ, Yue YL, Yang CG, Wang Y, Qin JQ, Zhang XY, Wu ZS. Ultrarapid synthesis Ni-Cu bifunctional electrocatalyst by self-etching electrodeposition for high-performance water splitting reaction. Appl Surf Sci. 2021; 561: 150030.

[5] Guo J, Ouyang C, Zhan Z, Lei T, Yin P. Facile synthesis of tubular CoP as a high efficient electrocatalyst for pH-universal hydrogen evolution. Int J Hydrogen Energy. 2022; 47:181-196.

[6] Wang Z, Wang Y, Xiao W, et al. Ru, B Co-doped hollow structured iron phosphide as highly efficient electrocatalyst toward hydrogen generation in wide pH range[J]. J Mater Chem A. 2022; 10(28): 15155-15160.

[7] Lai Y, Xia W, Li J, Pan J, Jiang C, Cai Z, Huang XL, Wang T, He JP. A confinement strategy for stabilizing two-dimensional carbon/CoP hybrids with enhanced hydrogen evolution. Electrochim Acta. 2021; 375: 137966.

[8] Gebreslase GA, Martínez-Huerta MV, Sebastián D, Lázaro MJ, NiCoP/CoP sponge-like structure grown on stainless steel mesh as a high-performance electrocatalyst for hydrogen evolution reaction, Electrochim Acta, 2023; 438: 141538